HEFAT2012
9th International Conference on Heat Transfer, Fluid Mechanics and Thermodynamics
16 – 18 July 2012
Malta

WATER DROPLET EVAPORATION AT HIGH PRESSURE AND TEMPERATURE LEVELS – PART II: COMPARISON OF EXPERIMENTAL RESULTS WITH A 1D SIMULATION

Barabas B.*, Kefalas A., Schnitzler J. P., Benra F.-K., Dohmen H.-J.
*Author for correspondence
Department of Mechanical Engineering,
University of Duisburg-Essen,
47058 Duisburg,
Germany,
E-mail: botond.barabas@uni-due.de

ABSTRACT

Water injection into gas turbines is subject of investigations since decades, due to a high power and efficiency augmentation potential compared to the simple gas turbine cycle. Based on former research at ambient conditions, some technologies have already been realized, e.g. inlet fogging. Further applications of water injection at higher temperature and pressure levels are limited, because of few experimental data. In order to gain fundamental understanding at these boundary conditions, a novel test facility for droplet evaporation investigations has been built up at the Department of Mechanical Engineering at University of Duisburg-Essen. The resulting spray patterns are recorded by a laser based measuring technology, Phase Doppler Particle Analyzer (PDPA).

In this second part of the paper, experimental results from the test facility are compared to simulation results of a 1D-model for droplet evaporation. The focus of this investigation is on the accordance of the simulation results with the experimental data at high pressure and temperature levels.

INTRODUCTION

Two-phase flow is a topic of interest in modern gas turbine applications. The injection of water upstream of the first compressor stage, the so called wet compression, has a potential for power augmentation, due to the decreased compressor work and higher mass flow. It is most effective at hot and dry ambient conditions [1], because at these conditions the most amount of water vapor can be absorbed by the air. The influence of wet compression on the engine characteristics has been examined in some studies numerically ([2] - [4]).

However, wet compression supersaturates the inlet air; hence water droplets remain in the flow. The behavior of single water droplets, especially their evaporation, at low pressures and low temperatures, as they can be found in the first stages of the compressor, has been topic of some investigations in the past. A numerical investigation of droplet evaporation at low pressures and temperatures has been performed by Matz et al. [5]. They found out that the heat up time of a single droplet is very short compared to the total evaporation time. Chaker et al. [1] simulated single droplet evaporation at three different ambient conditions. They found out a linear dependence of the evaporation time on the initial droplet diameter.

To the authors knowledge, experimental investigations of droplet behavior injected in a hot gas flow at elevated temperature and pressure levels, as they can be found in rear compressor stages, have not been topic of studies yet. To investigate this behavior a novel test facility has been built up at the Department of Mechanical Engineering at University of Duisburg-Essen.

After the build-up phase, which is described in Schnitzler et al. [6], the first measurements have been taken and evaluated by Kefalas et al. [7]. Based on these measurements a droplet evaporation model, first introduced by Abramzon and Sirignano [8], is extended for polydisperse sprays and droplet breakup.

In this paper the extended model is compared to the basic version and to experimental data at elevated pressure- and temperature levels.

NOMENCLATURE

B_M	[-]	Spalding mass transfer number
B_T	[-]	Spalding heat transfer number
C_p	[kJ/(kg K)]	Specific heat at constant pressure
D_{32}	[µm]	Sauter mean diameter
D	[µm]	Diameter
D	[m²/s]	Diffusion rate
Δh_v	[kJ/kg]	Specific evaporation enthalpy
Δt	[s]	Timestep

F_M	[-]	Mass transfer correction factor due to Stefan flow
ϕ	[-]	Exponent parameter
$\dot{m}$	[kg/s]	Mass flow rate
On	[-]	Ohnesorge number
$\dot{Q}$	[kJ/s]	Heat flow
ρ	[kg/m³]	Density
r	[m]	Radius
Re	[-]	Reynolds number
Sc	[-]	Schmidt number
Sh	[-]	Sherwood number
SMD	[µm]	Sauter mean diameter
T	[K]	Temperature
We	[-]	Weber number
x	[m]	Streamwise direction
Y	[-]	Mass fraction

Subscripts

0	Initial
d	Droplet
g	Gas/ main flow
s	Surface
W	Water
∞	Gas film

EXPERIMENTAL TEST FACILITY

The novel test facility for droplet evaporation investigations at elevated pressure and temperature levels is located in the laboratories at the Department of Mechanical Engineering at University of Duisburg-Essen. It is designed to conduct laser based measurements of water nozzle sprays with boundary conditions of the main flow up to 673K and 1MPa.

Figure 1 gives an overview of the test facility. Ambient air is compressed with an intercooled 4-stage-radial compressor (1). An electric heater (2) is located downstream of the compressor to heat up the main flow, before it reaches the measuring section (3), a 1m long glass tube with an inner diameter of 102mm. The water injection nozzle (4) is located in the center at the beginning of the measuring section. The water spray is accessed optically with a Phase Doppler Particle Analyzer (PDPA) system. A bypass (5) can be used to adjust the main flow velocity in the measurement section in a wide range at constant temperature and pressure conditions. Further descriptions of the test facility are given in Schnitzler et al. [6] and Kefalas et al. [7].

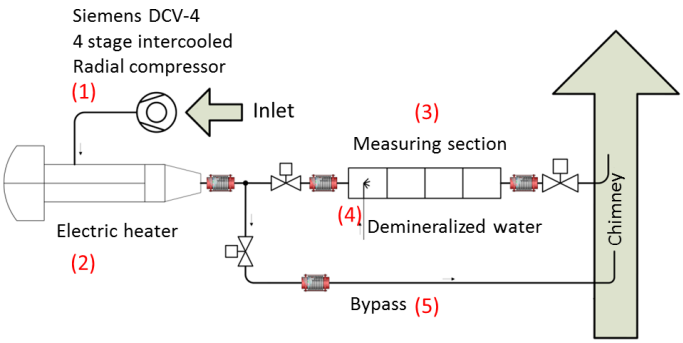

Figure 1: Schematic of the novel droplet evaporation test facility.

The boundary conditions, as they were applied in the experiment and the simulation are presented in Table 1. The experimental values vary in a range of ±0.5% additionally to the measurement uncertainties, due to oscillations of the electric heater control.

		Experiment	Simulation
Main flow temperature	[K]	465.9	463
Main flow pressure	[MPa]	0.42	0.41
Average main flow velocity	[m/s]	63	65
Water temperature	[K]	284	289
Injected water mass fraction	[%]	1.71	1.73

Table 1: The boundary conditions of the experiment and the simulation.

DESCRIPTION OF THE NUMERICAL MODEL

The model in this paper is based on the droplet evaporation model of Abramzon and Sirignano [8]. It has been extended for polydisperse sprays and droplet breakup, which are described in the following section.

In the basic model (Model A), a spray of identical droplets, without breakup and agglomeration is assumed. The droplets are modeled as perfect spheres with uniform temperature and equal diameters. A gas film is assumed around each droplet to model the resistance to heat and mass exchange between the droplet surface and the main flow. The gas and water properties are based on the Kretzschmar Property Libraries [9].

Abramzon and Sirignano describe the evaporation mass flow rate for a single droplet by

$$\dot{m}_d = 2\pi\bar{\rho}_g \bar{D}_{dg} r_d Sh^* \ln(1+B_M)\,. \qquad (1)$$

$\bar{\rho}_g$ and $\bar{D}_{dg}$ are the average density of the vapor in the gas film and the averaged diffusion rate between the droplet and the main flow, respectively. r_d is the droplet radius. The Spalding mass transfer number B_M is calculated as

$$B_M = \frac{Y_{Ws} - Y_{W\infty}}{1 - Y_{Ws}}\,, \qquad (2)$$

with the water mass fraction at the droplet surface (Y_{Ws}) and in the surrounding gas film ($Y_{W\infty}$).

The modified Sherwood number Sh^* is expressed as

$$Sh^* = 2 + (Sh - 2)/F_M\,, \qquad (3)$$

with F_M as a correction factor representing the change of the gas film thickness due to the Stefan flow. The Sherwood number Sh is defined as the non-dimensional mass transfer coefficient

$$Sh = 1 + (1 + \mathrm{Re} \cdot Sc)^{\frac{1}{3}} \cdot f(\mathrm{Re}). \quad (4)$$

To calculate the heat flow into the droplet the following equation is used:

$$\dot{Q}_d = \dot{m}_d \left[\frac{C_{pW}(T_g - T_d)}{B_T} - \Delta h_v \right]. \quad (5)$$

The Spalding heat transfer number B_T is calculated iteratively from

$$B_T = (1 + B_M)^{\phi} - 1, \quad (6)$$

with ϕ as a parameter dependent on B_T.

Model B is based on Model A but calculates the heat and mass transfer equations parallel for more than one droplet diameter within a timestep. The initial droplet diameter distribution is taken from the experimental results. It is assumed that the droplets do not influence each other. Therefore, the current heat and mass transfer rates between each droplet size and the main flow are calculated with the same main flow properties. After a timestep loop, the new main flow properties are calculated as an average value.

Model C incorporates additionally a droplet breakup model. It is based on the work of Schmehl et al. [10] with some additions and simplifications:

- Only one of the three breakup mechanism is considered.
- Only a single secondary droplet size is assumed to result from the breakup. A part (25%) of the broken-up droplets is assumed as instantly evaporated.
- Based on a calculated characteristic breakup time, the breakup per timestep is set in relation to that characteristic time.

The decision to consider only one breakup mechanism is, because a single correlation (equation (7)) for secondary droplet sizes, which covers all three mechanisms, exists. For simplification reasons, the resulting droplet diameter is assumed to equal the SMD, as defined in equation (8). The partly instantaneous evaporation should reflect the very small droplet diameters that result from the breakup process and evaporate instantly. The rate is set to 25%.

Breakup is assumed for a droplet diameter class if the Weber number We, which is a function of the relative velocity between the main flow and the droplet, exceeds a specific value:

$$We > 12 \cdot \left(1 + 1.077 \cdot On^{1.6}\right). \quad (7)$$

The relative velocity is calculated within the model with the individual drag coefficient of each droplet diameter class every timestep.

The resulting droplet diameter is assumed as the characteristic secondary droplet SMD:

$$D_{32} = D_0 \cdot 6.2 \cdot On^{0.5} \cdot We^{-0.25}. \quad (8)$$

Comparison of the models with each other

The SMD normalized with the initial SMD of the three different models is plotted over the streamwise distance in Figure 2. The SMD is calculated in the entire paper with droplets' diameter bigger than 10µm. The initial conditions for all simulations are the same and given in Table 1.

The different model approaches are clearly visible. The SMD of Model A decreases monotonously from the injection point, due to the single droplet class, on which the model is based. During the evaporation process the diameter of the droplet decreases. In contradiction, the SMD of Model B, which consists of different droplet sizes, increases monotonously from the beginning. In this model the smaller droplets evaporate faster than the bigger droplets, due to their higher surface-to-volume ratio. Thus the SMD increases. The SMD of Model C shows a sharp decrease in the vicinity of the injection nozzle. Further downstream the SMD increases. The droplet breakup algorithm causes the decrease of the SMD in the vicinity of the nozzle. The small steps visible in the graph of Model C occur when a droplet class diameter falls below 10µm, the limit for SMD calculations.

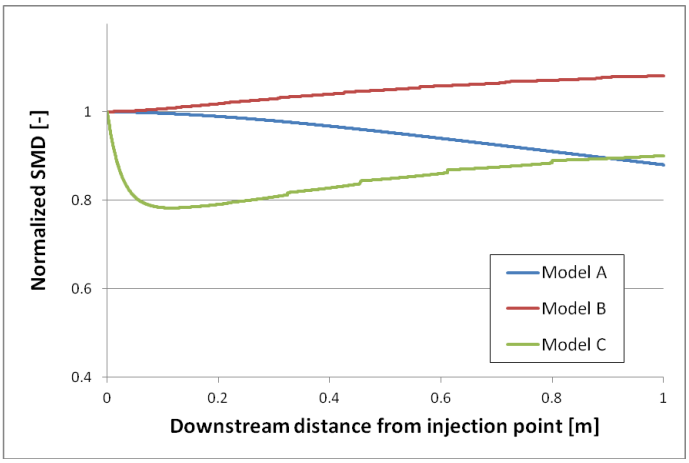

Figure 2: Normalized SMD plotted over the streamwise length. Results of the three different models compared with each other.

Figure 3 presents the non-evaporated water mass normalized with the injected water mass over the streamwise length. In the vicinity of the nozzle (x < 0.2m), Model C has the highest evaporation rate, due to the partly evaporation at the droplet break up. Thus, in this region the non-evaporated water mass is the lowest in comparison to the other models. Further downstream, when the breakup process is finished, the non-evaporated water mass of Model B and Model C converge each other. This is due to polydisperse spray assumption of both models. In contradiction to that, the non-evaporated water mass of Model A decreases faster than the one of the two other models in the rear part of the simulated measuring section (x > 0.6m). The reason is the increasing surface-to-volume ratio and therewith higher evaporation rate of the droplets simulated in Model A.

The prediction of the non-evaporated water mass within the first meter behind the injection point is less sensitive to the

specific model than the SMD is. The assumed evaporation due to breakup in Model C plays a minor role than it influences the SMD. Hence, if the focus of a numerical investigation is laid on the evaporation rate only, the faster and more simple Model A fulfills the demands on accuracy within a streamwise distance of x = 0.5m.

However, in this paper the SMD is a topic of interest, too, thus in the following only Model C, which incorporates the most physical assumptions of all three models, is compared to the experimental results.

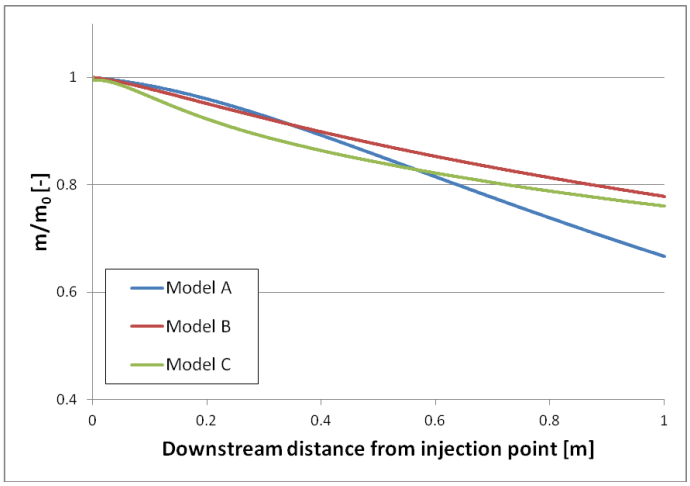

Figure 3: The normalized non-evaporated water mass plotted over the streamwise length. Results of the three different models compared with each other.

NUMERICAL RESULTS

The influence of different numbers of initial diameter classes on the SMD, simulated with Model C, is presented in Figure 4. The SMD normalized with the initial SMD is plotted over the streamwise distance. The calculation with the lowest number of diameter classes (5 classes) shows a significant difference compared to the calculations with more diameter classes (34, 68, 136, and 260 classes). Though, the difference of the normalized SMD is only slightly dependent on the diameter class if its number is higher than 34. However, in the simulation with 34 classes, the steps, at which the diameter has gone below the SMD calculation limit of 10µm, are more distinct than in the calculations with more (68, 136, and 260) diameter classes. The calculation with 68 classes gives the best compromise between the quality of the results and the required calculation time. Hence, the following calculations are set up with 68 initial diameter classes.

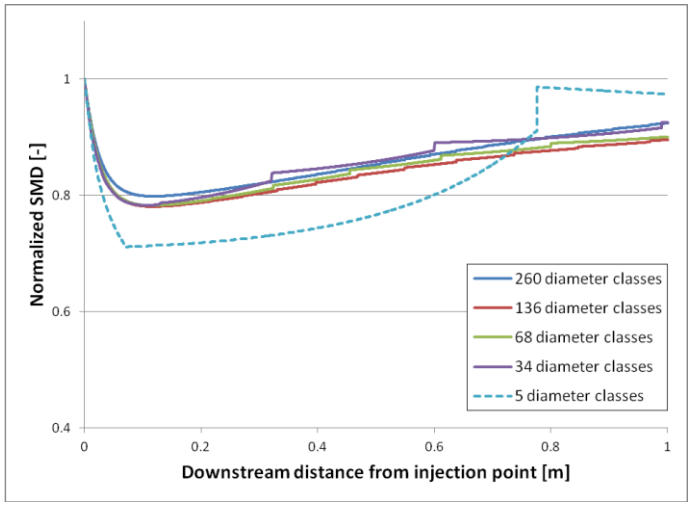

Figure 4: Dependence of the SMD results of Model C on a diameter class variation.

The dependence of the normalized SMD on different timesteps is presented in Figure 5. It is evident that the timestep has no influence on the normalized SMD. Thus, the longest timestep ($\Delta t = 1 \cdot 10^{-5}$ s) is chosen for further calculations, to achieve the shortest calculation time. It should be noted that a longer timestep than the chosen one effects in a numerical crash of the simulation.

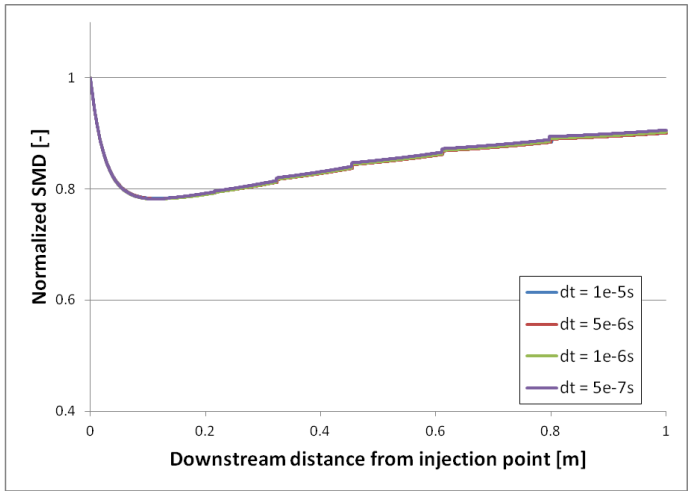

Figure 5: Dependence of the SMD results of Model C on a timestep variation.

Comparison of the SMD in experiment and simulation

The SMD gives a fast overview of the thermodynamic potential of a droplet spray. Small SMD correspond to large surface-to-volume ratios, thus to a high evaporation rate. However, for more detailed information the diameter distributions should be considered.

The SMD of the numerical calculations and the experiments, normalized with the initial SMD, are plotted over the streamwise length in Figure 6. In the vicinity of the nozzle exit both the measured and the numerical results show a sharp decrease of the SMD. The decrease in the experimental results

is more intensive than the one in the calculation. This disagreement could be due to a more complex breakup mechanism than it is assumed in the model. Beside the considered primary to secondary droplet break up, the atomization of the injected water film is ignored. Nevertheless, the water film prior the atomization can neither be measured with the PDPA system. It is only able to measure droplets and particles [7]. Thus, the experimental results have to be considered with caution in this region (x < 0.1m), too. The results of the non-evaporated water mass in Figure 7 support this assumption. It can be concluded from this comparison that the breakup algorithm of the model has to become faster and harsher.

Further downstream from the breakup region (x > 0.1m), the SMD, measured in the experiments and calculated numerically, show a similar trend. Both increase slightly towards downstream direction. The measured SMD is marginally higher than the calculated one, but this difference decreases towards downstream direction. At the end of the measuring section at x = 1m they reach a SMD of about 90% of the initial value.

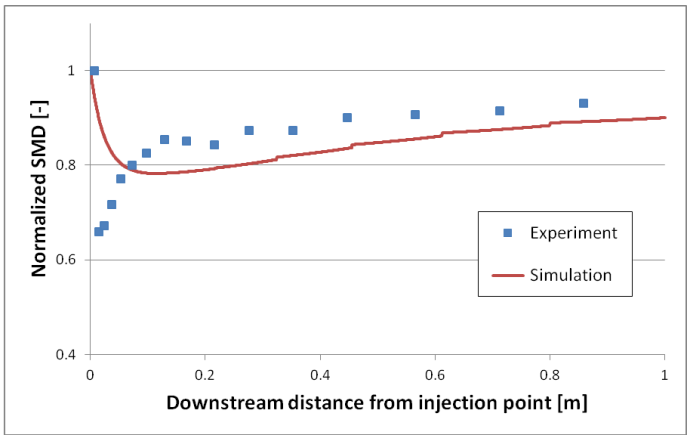

Figure 6: Comparison of the SMD from the experimental results (blue squares) with the numerical ones (red line) at a hot gas temperature of 463K and pressure of 0.41MPa.

Comparison of the non-evaporated water mass in experiment and simulation

In Figure 7 the normalized non-evaporated water mass over the streamwise direction is presented. The numerical values are normalized with the initially injected water mass. In contradiction, the experimental values are normalized with the maximum value at x = 0.13m, due to the assumption that in the vicinity of the nozzle (x < 0.1m) a water film exists, which cannot be measured by the PDPA system. The even higher measured mass flow at x = 0.28m is treated as an outlier. The error of this approximation lies in order of the evaporated water between x = 0m and x = 0.13m. Thus, the real mass flow is slightly overestimated.

Except the disagreement in the vicinity of the nozzle, both curves fit quantitatively and qualitatively to each other. The numerical results seem to underpredict marginally the amount of non-evaporated water. A clear disagreement between numerical and experimental results can only be observed, as described, in the vicinity of the nozzle (x < 0.1m). A comparison between the water mass flow measured with the PDPA system and the flow meter, installed in the water feed pipe, could give a better basis to validate the evaporation model. Unfortunately, the measurement of the absolute water mass flow is very difficult with a PDPA system due to the exact determination of the measuring volume.

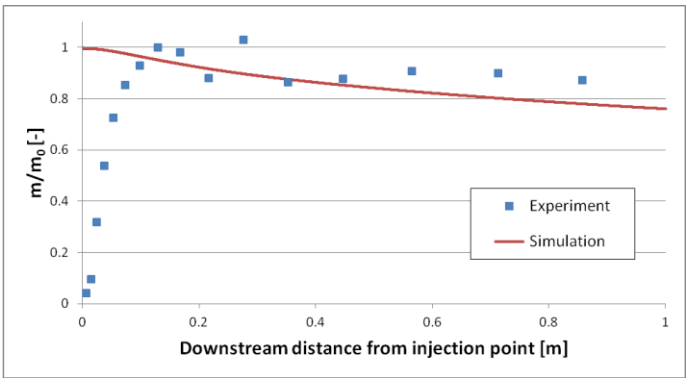

Figure 7: Comparison of the normalized non-evaporated water mass. Experimental results (blue squares) and numerical ones (red line) at a hot gas temperature of 463K and hot gas pressure of 0.41MPa.

Comparison of the diameter distribution at different axial positions in experiment and simulation

The cumulative diameter distributions at different axial downstream positions summed up over an orthogonal plane are plotted in Figure 8. Obviously the gaps between the measured and the simulated distributions get larger towards downstream direction. The droplet sizes in the simulation become smaller, whereas the measured sizes increase, towards downstream direction. The significant agglomeration of small droplets at an axial position of x = 0.86m could be due to the model assumption that the droplet size decreases continuously before they finally evaporate.

The mismatch between the experimental and the simulation results is an incentive to improve the model. Especially the behavior of small droplets has to be reconsidered. They accumulate in the model, whereas they disappear in the measurements towards downstream direction. Two possible solutions could help: Extending the model with a droplet agglomeration algorithm. Though, agglomeration seems to be unlikely to happen in reality; the droplets are too far away from each other. More probable, the heat and mass transfer for small droplets might be higher than currently assumed. The evaporation rate for them seems to be not modeled high enough. Therefore, their occurrence in the model results is higher than measured in the experiment.

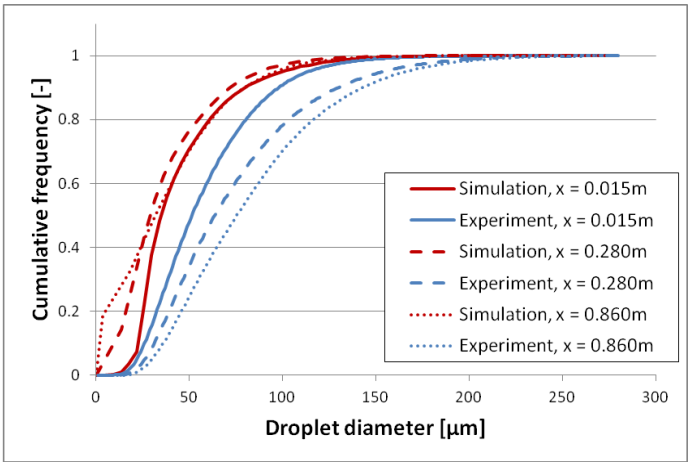

Figure 8: Comparison of the cumulative droplet distributions at different axial positions. Blue: Simulation. Red: Experiment. Solid line: x = 0.015m, dashed line: x = 0.28m, dotted line: x = 0.86m.

SUMMARY AND CONCLUSIONS

The basic 1D evaporation model of Abramzon and Sirignano [8] has been extended with droplet breakup and different diameter classes. The comparison of the different models with each other showed a big influence on the calculated SMD over the streamwise direction, but, only a slight influence on the prediction of the non-evaporated water mass. The most advanced model was compared to experimental data gathered at the novel droplet evaporation test facility at the Department of Mechanical Engineering at University of Duisburg-Essen. The boundary conditions for the comparing experiment were at elevated temperature (466K) and pressure (0.42MPa) levels. The extended evaporation model showed a poor agreement in the vicinity of the nozzle for the SMD and the non-evaporated water but a good agreement further downstream. The implementation of droplet breakup will need an improvement in the model, since it seems to happen too slowly and not intensively enough. Based on the measured values, smaller secondary droplet sizes might be expected. On the other hand the precision of the PDPA measurements in the vicinity of the nozzle should be considered, too, because if a water film was existent it could neither be measured. The difference between the experimentally and numerically gathered droplet distributions increases towards downstream direction. A more thorough investigation has to be laid on the evaporation of small droplets in future. The assumed heat- and mass transfer equations in the model seem to be too low for small droplets.

However, the extended 1D model is a good basis to predict evaporation at elevated temperature and pressure levels. In future, when further measurements of the test facility are available, the model can be fine-tuned especially in the vicinity of the injection point to give even better results.

REFERENCES

[1] Chaker M.A., Meher-Homji C.B., Mee T., Inlet Fogging of Gas Turbine Engines – Experimental and Analytical Investigations on Impaction Pin Fog Nozzle Behavior, *Proceedings of ASME Turbo Expo 2003*, GT2003-38801, Atlanta, Georgia, USA

[2] Bhargava R. K., Bianchi M., Chaker M., Melino F., Peretto A., and Spina P.R., Gas Turbine Compressor Performance Characteristics During Wet Compression – Influence of Polydisperse Spray, *Proceedings of ASME Turbo Expo 2009*, GT2009-59920

[3] Bianchi M., Melino F., Peretto A., Spina P.R., and Ingistov S., Influence of Water Droplet Size and Temperature on Wet Compression, *Proceedings of ASME Turbo Expo 2007*, GT2007-27458, Montreal, Canada

[4] Bianchi M., Chaker M., de Pascale A., Peretto A., and Spina P.R., CFD Simulation of Water Injection in GT Inlet Duct Using Spray Experimentally Tuned Data: Nozzle Spray Simulation Model and Results for an Application to a Heavy-Duty Gas Turbine, *Proceedings of ASME Turbo Expo 2007*, GT2007-27361, Montreal, Canada

[5] Matz C., Kappis W., Cataldi G., Mundinger G., Bischoff S., Helland E., Ripken M., Prediction of Evaporative Effects Within the Blading of an Industrial Axial Compressor, *Proceedings of ASME Turbo Expo 2008*, GT2008-50166, Berlin, Germany

[6] Schnitzler J.P., Feng J., Benra F.-K., Dohmen H.J., and Werner K., Test Rig Design for Investigations of Water Droplet Evaporation at High Pressure and Temperature Levels, *Proceedings of the 14th International Symposium on Transport Phenomena and Dynamics of Rotating Machinery (ISROMAC-14)*, February 27th-March 2nd, 2012, Honolulu, HI, USA

[7] Kefalas A., Barabas B., Schnitzler J.P., Benra F.K., Dohmen H.-J., Water Droplet Evaporation at High Pressure and Temperature Levels – Part I: Experimental investigations of the spray pattern in dependence on parameter variation, *Proceedings of the 9th International Conference on Heat Transfer, Fluid Mechanics and Thermodynamics (HEFAT2012)*, Malta

[8] Abramzon B. and Sirignano W.A., Droplet vaporization model for spray combustion calculations, *International Journal of Heat and Mass Transfer*, Vol. 32, 1989, pp. 1605-1618

[9] Kretzschmar H.-J., Stöcker I., Hochschule Zittau/Görlitz, Fachgebiet Technische Thermodynamik, http://thermodynamik.hs-zigr.de/cmsfg/Stoffwertbibliothek/index.php?rubric=Stoffwertbibliothek (Accessed: 2012-02-01)

[10] Schmehl R., Klose G., Maler G., and Wittig S., Efficient Numerical Calculation of Evaporating Sprays in Combustion Chamber Flows, *RTO MP-14*, 1998